

# Fully Developed Turbulence and Intermittency.

U. FRISCH

CNRS, Observatoire de Nice - BP 139, 06003 Nice Cedex, France

## 1. – Simple ideas and misconceptions about turbulence.

Viscous incompressible 3-D flow can become turbulent when the Reynolds number  $R$  is sufficiently large. The latter is expressible, in terms of a typical scale  $L$  of the flow, a typical velocity  $V$  and the kinematic viscosity  $\nu$ , as the ratio of the viscous diffusion time  $L^2/\nu$  to the circulation (turn-over) time  $L/V$ . Information about turbulent flows comes from experiments, observations of nature and, increasingly, from computer simulations (cf. other lectures in this volume).

We now list and discuss some outstanding features of turbulent flows. In each case we begin with naive widely accepted statements and show that they can lead to misconceptions. We shall assume that the reader is at least moderately familiar with dynamical-system concepts (cf. the lectures by LIBCHABER, LORENZ and RUELLE in this volume and ref. [1-3]).

**1.1.** *Sharp transitions can occur when the Reynolds number is varied.* – Transitions from laminar to turbulent flows are discussed elsewhere in this volume. Very carefully controlled experiments on, *e.g.*, Rayleigh-Bénard convection have revealed a great variety of scenarios for the transition. In such experiments, when the flow becomes turbulent, it is often chaotic only in time and highly organized in space. In shear flows the transition may lead to much stronger chaos in both time and space via the 3-D destabilization of 2-D coherent structures (cf. the computer experiments by ORSZAG, PATERA and BRACHET reported in ref. [4] and [5] and the lectures by ORSZAG).

**1.2.** *The flow is unstable and unpredictable.* – A very weak perturbation introduced at some time  $t_0$  may rapidly result in a complete distortion of the detailed flow pattern. Thus the flow may not be predictable in deterministic terms for more than a short time. It is conceivable, however, that statistical properties (involving, *e.g.*, time averages) are stable and can be predicted (cf. the difference between predicting weather and climate).

What do we understand by a «very weak perturbation»? The simplest way is to take an infinitesimal perturbation; such a perturbation is governed by the linearized dynamical equations. The growth of infinitesimal perturbations is controlled by the maximal Lyapounov characteristic exponent (LCE)  $\lambda_m$  (ref. [6, 7] and the lectures of Ruelle). Loosely stated, the fastest growing perturbation goes for very large times like  $\exp[\lambda_m t]$ , where  $\lambda_m \geq 0$ . Chaotic (or intrinsically stochastic) dynamical systems have  $\lambda_m > 0$ . In practice this does not necessarily mean complete lack of predictability. Indeed, i) small but finite perturbations may at first grow exponentially but eventually saturate at rather low levels, ii) the positive LCEs correspond to those directions in which the separation of neighbouring trajectories grows exponentially. There are also negative LCEs corresponding to shrinking separations and hence to no lack of predictability. In fact, it is known that chaotic dynamical systems can have strongly predictable features; one example is the «noisy periodicity» discussed by LORENZ [8]. Dissipative dynamical systems (*e.g.* viscous Navier-Stokes flow) may have a set that attracts trajectories for  $t \rightarrow \infty$ . The phase space can be infinite-dimensional (it usually is if the flow is governed by a partial differential equation), still the attractor can be finite-dimensional. If the dimension is small, the flow has in a sense only a finite number of unpredictable features. There is experimental evidence that many turbulent flows have strongly coherent quite predictable structures (cf. other lectures in this volume and ref. [9]). It is of interest to try to measure the dimension of their attractors.

Dynamical-system theory is also telling us that a turbulent flow with prescribed geometry and Reynolds number need not have unique statistical properties. Just like a body resting on a table may have several positions of stable equilibrium, a dynamical system can have several attractors with distinct basins. For example, in transition experiments of the Rayleigh-Bénard type the statistical regime that is obtained may depend on the way the system is prepared (cf. the lectures by LIBCHABER).

**I'3. Trajectories of marked particles are unstable and unpredictable.** – We now consider not the flow in some abstract phase space but the trajectories of individual marked particles following the fluid motion in (2-D or 3-D) physical space. Let us denote by  $\mathbf{v}(t, \mathbf{r})$  the velocity field in Eulerian co-ordinates. Particle trajectories are determined by the following dynamical system

$$(1.1) \quad d\mathbf{r}(t, \mathbf{a})/dt = \mathbf{v}(t, \mathbf{r}(t, \mathbf{a})), \quad \mathbf{r}(0, \mathbf{a}) = \mathbf{a}.$$

If the flow is incompressible,  $\nabla \cdot \mathbf{v} = 0$  and the dynamical system is conservative, *i.e.* the mapping  $\mathbf{a} \mapsto \mathbf{r}(t, \mathbf{a})$  conserves the Lebesgue measure.

The interesting observation is that the dynamical system (1.1) may be chaotic without the velocity field being so. One simple known example is

the spatially periodic steady Arnold-Beltrami-Childress flow ( $A, B, C$  real)

$$(1.2) \quad V_1 = A \sin x_3 + C \cos x_2,$$

$$(1.3) \quad V_2 = B \sin x_1 + A \cos x_3,$$

$$(1.4) \quad V_3 = C \sin x_2 + B \cos x_1,$$

introduced by ARNOLD [10] and CHILDRESS [11] and studied by HÉNON [12]. It is easily checked that  $\mathbf{v} \times \text{curl} \mathbf{v} = 0$ . Hence this flow is an exact solution of the 3-D Euler equations. This solution being steady hardly qualifies as «turbulent». Still the numerical evidence is that streamlines (here identical with the trajectories of marked particles) are chaotic when  $ABC \neq 0$ . We thus have a sort of «Lagrangian turbulence»: drops of dye introduced into the flow will develop extremely intricate structures. Lagrangian turbulence of this sort can also take place in two dimensions provided that the velocity field becomes time-dependent (periodic is enough). A very simple example is given by AREF [13]: in a circular shallow tank the fluid is agitated  $T$ -periodically by a stirrer (assumed to act like a point vortex); during a time interval  $T/2$  the stirrer is placed at some point  $M$  and then for another half-period at the diametrically opposite point  $M'$ . This simple device can give very efficient mixing.

The above observations about Lagrangian turbulence may be relevant to atmospheric predictability: the motion of an advected long-lived small-scale structure (say a radioactive cloud) in a large-scale 2-D flow can be unpredictable as soon as the large-scale flow is not steady.

**1.4. Turbulent flow enhances transport.** – In a nonturbulent fluid the transport of heat, momentum, etc. is caused by molecular motion and collisions: at scales much larger than the mean free path  $\lambda$ , a molecular-diffusion process takes place with a diffusion coefficient  $k_{\text{mol}} \sim \lambda v_{\text{th}}$ , where  $v_{\text{th}}$  is the r.m.s. thermal velocity. In a 3-D turbulent fluid with integral scale  $l_0$  and r.m.s. turbulent velocity  $v_0$  one can similarly construct a turbulent diffusion coefficient  $k_{\text{turb}} \sim \sim l_0 v_0$  usually  $\gg k_{\text{mol}}$ . The enhancement of transport by turbulence is sometimes the only evidence that a flow is turbulent (*e.g.* in the interiors of stars).

Steady 3-D flow with chaotic streamlines (such as the flow discussed above) will not usually produce turbulent diffusion. The reason is that the dynamical system defined by the streamlines will have Kolmogorov-Arnold-Moser (KAM) invariant surfaces within which marked particles remain trapped. Introducing some molecular diffusion amounts to letting the marked particles perform an additional Brownian motion by which they can escape from the KAM surfaces. Diffusive behaviour is then recovered at large scales.

We also stress that turbulent-transport coefficients are appropriate only for phenomena on scales much larger than  $l_0$ . This restriction is frequently

ignored in empirical modelling of turbulent flows. One example is the use of eddy viscosities in subgrid scale modelling in connection with computer simulations when it is not practical to resolve all the relevant scales. Such procedures may yield reasonable results when used in a dimensionally consistent way. They may also badly fail. The most obvious pitfall is that by increasing the viscosity the flow can be made laminar. The opposite can also happen: in Taylor-Couette flow and mixing layers transitions can occur such that, when  $R$  is increased, the large-scale flow becomes *more* coherent, while the small scales remain chaotic.

This may be somewhat similar to the existence of laminar windows for the control parameter within the chaotic domain observed, *e.g.*, in iterated maps [14]. In such a situation subgrid scale calculations may be unable to predict the coherence of the flow.

There are circumstances in which turbulence on a scale  $l_0$  acts to *enhance* rather than to diffusively damp the amplitude of the quantity being transported on a scale  $\gg l_0$ . In 2-D incompressible flow negative eddy viscosities can be used to explain that the energy cascade proceeds from small to large scales (cf. ref. [15, 16] and the lectures by SADOURNY and TENNEKES). In a 3-D flow with nonvanishing helicity (= integral over space of  $\mathbf{v} \cdot \text{curl} \mathbf{v}$ ) large-scale magnetic fields are amplified due to the « $\alpha$ -effect» (cf. ref. [17] and the lectures by CHILDRESS).

15. *High-Reynolds-number turbulence has a wide range of scales.* – Fourier analysis of velocity signals from a probe in high-Reynolds-number flow (*e.g.* a turbulent jet) reveals the kind of spectrum shown in fig. 1. The energy spectrum follows a power law  $\propto k^{-m}$  ( $m \approx 5/3$ ) over a range of scales (*i.e.* inverse wave numbers) extending from the integral scale  $l_0$  to the dissipation

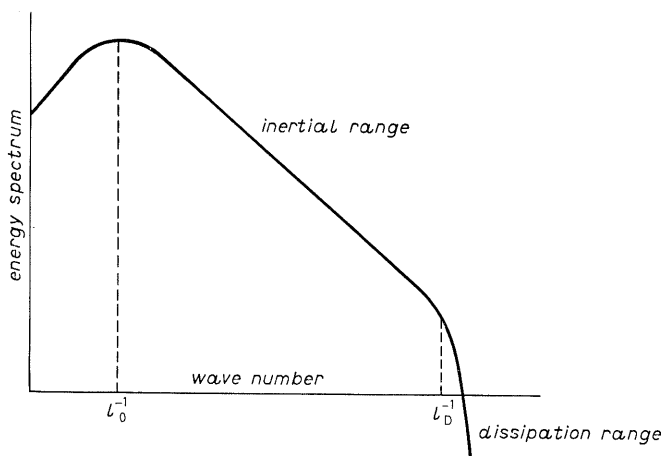


Fig. 1. – Energy spectrum of high-Reynolds-number turbulence. Double logarithmic co-ordinates.  $l_0$  is the integral scale and  $l_D$  is the dissipation scale.

scale  $l_D$ . The ratio  $l_0/l_D$  increases with  $R$  like  $R^n$  ( $n \approx 3/4$ ) and the small-scale motion is approximately isotropic. All this was predicted by KOLMOGOROV in 1941 [18]. Simple phenomenological interpretations can be given [19, 20]. The range of scales  $l \sim l_0$  is called the energy-carrying or production range, because that is where most of the turbulent energy is produced (usually by some instability mechanism). The range  $l_0 \gg l \gg l_D$  is the inertial range, because the dynamics are here dominated by the inertial terms in the Navier-Stokes equations (direct production and dissipation are negligible). The range  $l \lesssim l_D$  is called the dissipation range because both inertial and dissipation terms are relevant. A frequent misconception is that only dissipation is relevant (cf. ref. [21]). The increasing range of scales as  $R$  is increased does not itself imply that the number of basic degrees of freedom (those governing the attractor of the flow) is increasing. As stressed, for example, in Tennekes' lectures,

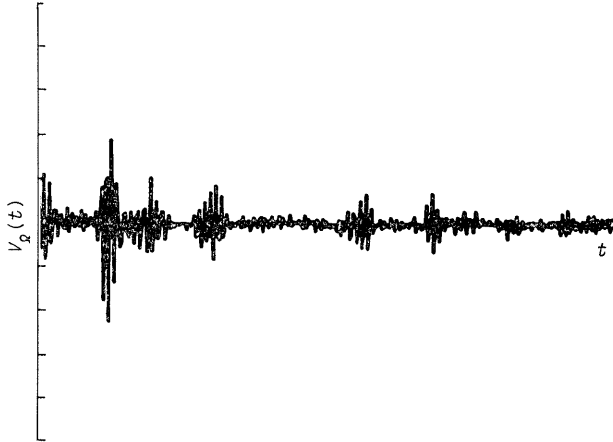


Fig. 2. — Intermittent velocity signal. The plot shows high-pass filtered output of a hot-wire probe measuring the velocity in grid-generated turbulent flow (Y. GAGNE, Institut de Mécanique de Grenoble).

turbulent flows are full of coherent structures. Presumably a chaotic process (that may have an attractor of relatively low dimension) controls the formation of such structures. It is conceivable that the formation of small scales by subsequent flattening of the structures into, *e.g.*, ribbons or sheets is governed by a predictable deterministic process. This picture is consistent with a low-dimensional attractor at high Reynolds numbers. Alternatively, and more likely, there may be additional small-scale instabilities (inviscid or viscous) leading to increasing chaos.

High-pass filtering of turbulent signals reveals that the small-scale activity is intermittent; it comes in bursts, as shown in fig. 2. This is already conspicuous in the inertial range and even more so in the dissipation range. Intermittency

was discovered by BATCHELOR and TOWNSEND [22]. Inertial-range intermittency has not yet received any systematic explanation; it is not consistent with the original 1941 Kolmogorov theory (often referred to as K 41) and has led to various modified theories [20, 23-25]; we shall come back to this in sect. 2 and the appendix. Dissipation range intermittency is much better understood and can be related to singularities of the solutions of the Navier-Stokes equations at complex times (cf. ref. [21, 26]); an interesting early interpretation of this intermittency may be found in ref. [27]. The essence of the explanation is that high-pass filtering of an analytic function with complex-time singularities produces bursts centred at the real part of the singularities and with an overall amplitude proportional to  $\exp[-\Omega|\tau|]$ , where  $\Omega$  is the filter frequency and  $\tau$  the imaginary part of the singularity. The (rare) singularities closest to the real axis are strongly favoured for large  $\Omega$ .

## 2. – Fully developed turbulence: intermittency as a broken symmetry.

By fully developed turbulence (FDT) we understand the asymptotic regime that is obtained by letting the Reynolds number tend to infinity. We shall here consider only the 3-D case; for the quite different 2-D case, see the lectures by SADOURNY and TENNEKES and ref. [15, 16]. In geophysical flows inertial ranges of three decades and more are not uncommon [28]. Laboratory experiments can display substantial inertial ranges [29]. Computer simulations of the full Navier-Stokes on a grid of  $256^3$  points have now reached the point where features of fully developed turbulence begin to be conspicuous [30, 31].

Attempts to construct a theory of FDT go back more than 40 years: a long history of frustrated attempts which we shall not review here [32, 33].

One central difficulty of FDT appears to be a broken symmetry. This has already been discussed in ref. [26]. The argument will here be just summarized. Consider the Navier-Stokes equations

$$(2.1) \quad \begin{cases} \partial_t \mathbf{v} + \mathbf{v} \cdot \nabla \mathbf{v} = -\nabla p + \nu \nabla^2 \mathbf{v}, \\ \nabla \cdot \mathbf{v} = 0 + \text{boundary and initial conditions.} \end{cases}$$

In the infinite-Reynolds-number limit ( $\nu \rightarrow 0$ ) the Navier-Stokes equations are formally invariant under all the groups of scaling transformations  $\mathcal{D}_h$

$$(2.2) \quad \mathbf{r} \rightarrow \lambda \mathbf{r}, \quad \mathbf{v} \rightarrow \lambda^h \mathbf{v}, \quad t \rightarrow \lambda^{1-h} t, \quad \lambda > 0,$$

with arbitrary similarity exponent  $h$ . Since the production of turbulence singles out the scale  $l_0$ , the flow cannot be globally invariant under  $\mathcal{D}_h$  (neither

in a deterministic nor in a statistical sense). Still, the invariance may hold asymptotically at scales  $l \ll l_0$ . This is precisely one of the postulates of the K 41 theory [18], the other one being the assumption that there is a finite rate of energy dissipation per unit mass; it then follows that the flow is statistically self-similar with exponent  $h = 1/3$ . This has important consequences for the (longitudinal) structure functions. The latter are defined by

$$(2.3) \quad \langle (\delta v(l))^p \rangle \equiv \langle (v(\mathbf{r} + \mathbf{l}) - v(\mathbf{r}))^p \rangle,$$

*i.e.* the  $p$ -th-order moment of the velocity increments over a distance  $l$  (the velocity component being measured parallel to  $\mathbf{l}$ ). For homogeneous isotropic turbulence the r.h.s. of (2.3) is a function only of  $l = |\mathbf{l}|$  and of  $p$ . (Asymptotic) self-similarity with  $h = 1/3$  implies that

$$(2.4) \quad \langle (\delta v(l))^p \rangle \propto l^{\zeta_p}, \quad \zeta_p = p/3, \quad l_0 \gg l \gg l_D.$$

For  $p = 2$  this is just another way of writing the celebrated  $k^{-5/3}$  law. The trouble is that eq. (2.4) is only marginally supported by experiment for small  $p$ 's and not at all for large  $p$ 's. Power law behaviour appears to hold, but not with  $\zeta_p = p/3$ . Fairly accurate measurements of the  $\zeta_p$  for  $p$  up to about 10 have been reported recently in ref. [29]. The experimental values of  $\zeta_p$  for three flows are given in table I (taken from ref. [29]).  $R_\lambda$  is the Reynolds number based on the Taylor microscale. Clearly the results indicate that self-similarity is broken. In ref. [26] we show that, since scale invariance corresponds to a noncompact group, it is more likely to be broken than, say, isotropy, which corresponds to the compact group of rotations.

TABLE I. - *Exponents of structure functions (taken from ref. [29]).*

$p$	2	3	4	5	6	7	8
$R_\lambda = 515$ (duct)	0.71	1	1.33	—	1.8	—	2.27
$R_\lambda = 536$ (jet)	0.71	1	1.33	1.54	1.8	2.06	2.28
$R_\lambda = 852$ (jet)	0.71	1	1.33	1.65	1.8	2.12	2.22
$p$	9	10	12	14	16	18	
$R_\lambda = 515$ (duct)	—	2.64	2.94	3.32	—	—	
$R_\lambda = 536$ (jet)	2.41	2.60	2.74	—	—	—	
$R_\lambda = 852$ (jet)	2.52	2.59	2.84	3.28	3.49	3.71	

A weaker assumption that may be consistent with the data (but not necessarily with the Navier-Stokes equations) is *conditional* self-similarity: one assumes, for example, a hierarchical embedding of bursts within bursts as one proceeds to ever smaller scales (cf. ref. [20, 25]). A number of such hierarchical intermittent models has been constructed with probabilistic elements introduced in an *ad hoc* way; according to such models, in FDT the energy dissipation is concentrated in a fractal set [34]. The fractal dimension  $D$  of this set can be inferred from the sixth-order structure function [20]. According to the recent data reported in ref. [29]  $D \approx 2.8$ ; this would indicate that dissipative structures are so extremely convoluted that they are nearly space filling ( $D = 3$ ). In the appendix, written with PARISI, we show that the data are consistent with a picture of intermittency involving more than one fractal set.

Explaining the broken self-similarity by the intermittency is just displacing the problem. There are recent indications that the broken-symmetry–intermittency problem of FDT has to do with chaotic dynamical systems. This is based on results obtained with the «two-component shell model» of ref. [35, 36]. Earlier shell models have been introduced in ref. [37] and studied in ref. [38-40]. The general idea is as follows. Let us start with 3-D Navier-Stokes turbulence. Fourier space for the space variable is divided into octave shells comprised between successive wave numbers  $k_n$  defined by

$$(2.5) \quad k_{-1} = 0, \quad k_0 = l_0^{-1}, \quad k_n = 2^n k_0 \quad (n \geq 1).$$

The total velocity field  $\mathbf{v}(t, \mathbf{r})$  can be decomposed into contributions  $\mathbf{v}_n(t, \mathbf{r})$  each of which involves  $O(k_n^2)$  Fourier components. In shell models it is assumed that each shell has only a small number of degrees of freedom which does not increase with  $n$ . The models are chosen to have many structural properties in common with the Navier-Stokes equations: form of linear and nonlinear terms, conservation of energy for  $\nu = 0$ , conservation of volume in phase space for  $\nu = 0$ , etc. Interactions are only between neighbouring shells (motivated by the observation that in 3-D FDT energy transfer involves mostly interactions between comparable scales). The two-component shell model reads (ref. [36])

$$(2.6) \quad \partial_t u_n = \alpha(k_n u_{n-1}^2 - k_{n+1} u_n u_{n+1} - k_n b_{n-1}^2 - k_{n+1} b_n b_{n+1}) + \\ + \beta(k_n u_{n-1} u_n - k_{n+1} u_{n+1}^2 - k_n b_{n-1} b_n + k_{n+1} b_{n+1}^2) - \nu k_n^2 u_n + \delta_{1n},$$

$$(2.7) \quad \partial_t b_n = \alpha k_n (u_{n+1} b_n - u_n b_{n+1}) + \beta k_n (u_n b_{n-1} - u_{n-1} b_n) - \nu k_n^2 b_n,$$

$$(2.8) \quad n = 1, 2, 3, \dots, \quad u_0 = b_0 = 0.$$

$\alpha$  and  $\beta$  are real parameters. The Kronecker  $\delta_{1n}$  provides a driving force for the first shell; higher-order shells are excited by nonlinear interactions. The



following properties are easily checked: 1) the nonlinear interactions conserve the total energy

$$(2.9) \quad E = \frac{1}{2} \sum_{n=1}^{\infty} (u_n^2 + b_n^2);$$

ii) when  $\nu = 0$  and only a finite number  $N$  of shells are kept (with  $u_{N+1} = b_{N+1} = 0$ ), the flow in the  $2N$ -dimensional space defined by eqs. (2.6), (2.7) is conservative, *i.e.*

$$(2.10) \quad \sum_{n=1}^N \left( \frac{\partial}{\partial u_n} (\partial_t u_n) + \frac{\partial}{\partial b_n} (\partial_t b_n) \right) = 0 \quad (\text{Liouville theorem}).$$

Similar properties hold for the Navier-Stokes equations (ref. [32, 33]). The two-component shell model was introduced by GRAPPIN, LÉORAT and POUQUET [35] as a generalization to MHD (conducting flow with magnetic field) of the model of Desnyansky and Novikov [37], to which it reduces when  $b_n \equiv 0$ . It is also possible to consider the two-component shell model as a model of the Navier-Stokes equations that retains two rather than one mode per shell. It is noteworthy that the Liouville theorem (eq. (2.10)) does not hold for the Desnyansky-Novikov model.

The main results obtained for the two-component shell model (ref. [36]) in the FDT limit ( $\nu \rightarrow 0$ ) are as follows:

a) If all the  $b_n$ 's are set equal to zero and if  $2^{1/3}\alpha - \beta > 0$ , the solutions of eqs. (2.6), (2.7) tend for  $t \rightarrow \infty$  to a « K 41 fixed point ».

b) For nonvanishing  $b_n$ 's intermittent chaotic solutions have been obtained (so far in a limited number of numerical experiments).

The precise meaning of statement a) is

$$(2.11) \quad \lim_{n \rightarrow \infty} \lim_{\nu \rightarrow 0} \lim_{t \rightarrow \infty} u_{n+1}/u_n = 2^{-1/3},$$

and similarly for the  $b_n$ 's. It is easily checked that all nonlinear terms in eqs. (2.6), (2.7) vanish when  $u_{n+1}/u_n = b_{n+1}/b_n = 2^{-1/3}$ . Stability of this K 41 solution is demonstrated by a linear stability analysis and by computer experiments. For nonvanishing  $b_n$ 's at high Reynolds numbers chaotic solutions (with positive maximum LCE) are observed, the high-shell  $u_n$ 's and  $b_n$ 's being conspicuously intermittent in time. Time averages of the quantities  $\langle (u_n(t))^p \rangle$ , analogous to structure functions, show power law dependence (in  $k_n$ ) with significant deviations from K 41 scaling (ref. [36]). Note that intermittent behaviour has been previously observed in shell models in which the energy dissipation is not through a linear term but through a nonlinear eddy viscosity [40, 41].

To understand how the intermittent chaotic behaviour comes about in shell models, there are at least two strategies. One can truncate the model

and study bifurcations controlled by the Reynolds number. This has already been done for the cases of two and three shells [36]. Alternatively one can work directly with infinitely many shells and infinite Reynolds number. Indeed, it is possible to construct a one-parameter family of models which in some ranges have K 41 solutions and in other ranges chaotic intermittent solutions. As the parameter is varied, bifurcations are expected which lead to symmetry breaking and chaos.

### 3. – Turbulence with a spectral gap and predictability (based in part on ref. [42]).

In the atmosphere of the Earth there is a number of instability mechanisms acting on very different scales: for example, the large-scale baroclinic instability and the small-scale convective instability. Under what conditions can the resulting turbulent flows coexist and be separated by a spectral gap (*i.e.* be spectrally segregated as depicted in fig. 3)? Many atmospheric scientists believe that there is such a gap in the atmosphere and it has been argued by LORENZ ([43] and this volume) that this can result in increased predictability of the weather.

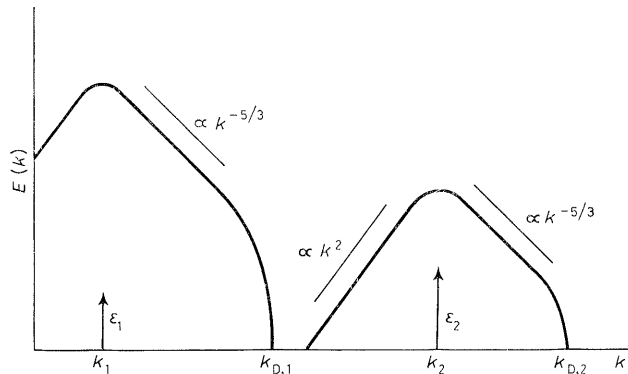


Fig. 3. – 3-D turbulence with a spectral gap.

The simplest model on which the possibility of a spectral gap can be examined is homogeneous isotropic turbulence with two distinct production mechanisms acting at scales  $l_1 = k_1^{-1}$  and  $l_2 = k_2^{-1} \ll l_1$ . To make the problem (somewhat) tractable it is essential to assume a wide separation of scales.

Before putting the two turbulences together, let us recall some additional facts about the spectrum of high-Reynolds-number homogeneous isotropic turbulence driven at a single scale, as shown in fig. 4. Subtleties such as intermittency corrections to K 41 will be mostly ignored, since they are probably not very relevant for what will follow. We denote by  $\epsilon_1$  the rate at which energy is injected per unit mass into the turbulent flow. Stationarity is assumed; hence  $\epsilon_1$  is equal to the rate at which energy cascades to smaller scales and

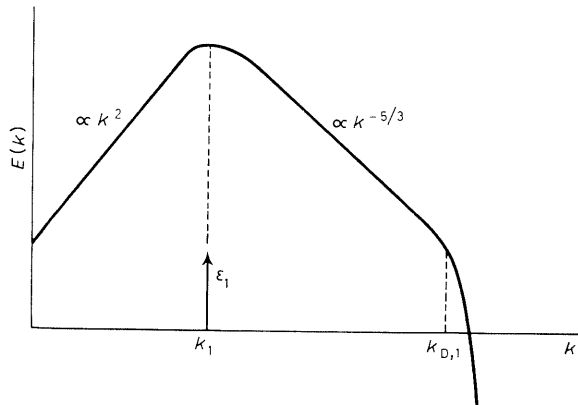


Fig. 4. – Inertial and equilibrium ranges of 3-D turbulence.

also equal to the rate of dissipation. The latter is  $2\nu\Omega_1$ , where  $\nu$  is the viscosity and  $\Omega_1$  the enstrophy (mean square vorticity). The former can be estimated in terms of  $l_1$  and the r.m.s. turbulent velocity  $v_1$ : the amount of energy in scales  $\sim l_1$  is  $\sim v_1^2$ ; the characteristic time for transferring this to smaller scales is the eddy turn-over time  $t_1 \sim l_1/v_1$ ; hence  $\varepsilon_1 \sim v_1^2/t_1 \sim v_1^3/l_1$ . The energy spectrum follows the Kolmogorov law

$$(3.1) \quad E(k) \sim \varepsilon^{2/3} k^{-5/3}$$

in the inertial range

$$(3.2) \quad k_1 = l_1^{-1} \ll k \ll k_{D,1} \sim k_1 R^{3/4},$$

where  $R \sim l_1 v_1/\nu$ . At small wave numbers,  $k \ll k_1$ , there is an «equilibrium range» in which

$$(3.3) \quad E(k) \propto k^2.$$

In this range there is an equipartition of kinetic energy between all Fourier modes (there are  $\sim k^2 dk$  modes with wave number between  $k$  and  $k + dk$ ). The equilibrium range is fed by beating-type interactions between two eddies in the energy-containing range, this being balanced by an eddy viscosity also coming mostly from the energy range [44]. In field-theoretic jargon the equilibrium range has «asymptotic infra-red freedom» (this is a school of physics!) as can be demonstrated using renormalization group methods [45, 46].

We are now in a position to understand the interactions of two turbulent motions separated by a gap (fig. 3). Let us denote by  $\varepsilon_i \sim v_i^3/l_i$  the energy production rates and by  $k_i = l_i^{-1}$  the energy-carrying wave number for the large-scale flow ( $i = 1$ ) and the small-scale flow ( $i = 2$ ). The main effect fo

the small scales on the large ones is to replace the molecular viscosity  $\nu$  by an eddy viscosity  $\nu_t \sim l_2 v_2$  (cf. subsect. 1'4). Thus the large-scale Reynolds number is reduced to an effective  $R_1^{\text{eff}} \sim l_1 v_1 / l_2 v_2$ . We denote by  $E_2(k)$  the energy spectrum that would be established with only small-scale production and by  $E_1(k)$  the spectrum that would be established with only large-scale production but with  $\nu_t$  used instead of  $\nu$ . The viscous cut-off for  $E_1(k)$  is at  $k_{D,1} \sim k_1 (R_1^{\text{eff}})^{3/4}$ . A necessary condition for spectral segregation is that  $k_{D,1} \ll k_2$ . This is easily seen to be equivalent to

$$(3.4) \quad \varepsilon_1 \ll \varepsilon_2 \quad \text{or} \quad v_1^3 / l_1 \ll v_2^3 / l_2 .$$

We have assumed up to this point that the small-scale turbulence is mostly unaffected by the presence of the large-scale turbulence. This requires that the turn-over time  $t_2$  be small compared to the characteristic time for distortion by large-scale shears, namely  $t_s \sim \Omega_1^{-1/2}$ . It is easily checked that the second condition gives the same relation eq. (3.4) as before. Finally we shall require that the large-scale turbulence should have a large effective Reynolds number  $R_1^{\text{eff}} \gg 1$ . Putting everything together, we get the conditions for spectral segregation of two fully developed 3-D turbulent flows

$$(3.5) \quad (l_1/l_2)^{-1} \ll v_1/v_2 \ll (l_1/l_2)^{1/3} .$$

If the left inequality becomes violated, the large-scale flow can become laminar (by the action of the small-scale turbulence!). A somewhat more quantitative study of this problem can be done using closure theory [42].

When intermittency is included in the above analysis (in the sense of ref. [20]), it is found that the exponent 1/3 in the r.h.s. of eq. (3.5) is lowered to  $(D-2)/3$ , where  $D$  is the fractal dimension of dissipation.

MCLAUGHLIN, PAPANICOLAOU and PIRONNEAU [47] have studied by asymptotic methods a variant of the spectral-gap problem in which the large- and small-scale flows are not driven and decay. So does the eddy viscosity and, eventually, molecular viscosity dominates. This may, however, take a very long time if the initial small-scale Reynolds number is large.

The above 3-D analysis is also easily extended to the coexistence of large-scale 2-D turbulence with small-scale 3-D turbulence. For this we must, of course, assume that there is a mechanism that keeps the large-scale flow 2-D. The situation is as shown in fig. 5.  $\beta_1$  is the rate of enstrophy production  $\beta_1 \sim (v_1^2/l_1^2)/(l_1/v_1) \sim v_1^3/l_1^3$ . The enstrophy inertial range extends from  $\sim k_1 = l_1^{-1}$  to  $\sim k_{D,1} \sim k_1 (R_1^{\text{eff}})^{1/2}$ , where  $R_1^{\text{eff}}$  is defined as before. By going through the same kind of analysis as before, we find the following conditions for spectral segregation of the two fully developed 2-D and 3-D flows

$$(3.6) \quad (l_1/l_2)^{-1} \ll v_1/v_2 \ll l_1/l_2 .$$

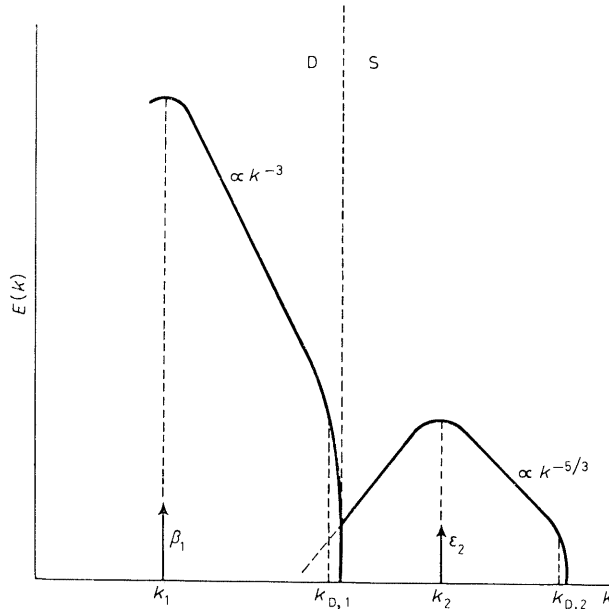


Fig. 5. – Spectral gap between large-scale 2-D turbulence and small-scale 3-D turbulence.

We now show that a spectral gap between small-scale 3-D turbulence and large-scale 2-D turbulence may lead to increased predictability of the large-scale motion (as suggested by LORENZ ([43] and this volume)). We assume that the flow can be resolved deterministically (D) up to a wave number in the spectral gap (indicated by a vertical dashed line in fig. 5) and that beyond the flow is only known statistically (S). According to ref. [48, 49] errors migrate from larger to smaller wave numbers. In a range where nonlinear interactions are mostly local (*e.g.* an inertial range), the characteristic time for error migration over, say, one octave of wave numbers is the local eddy turn-over time (what else could it be?). Across the spectral gap, however, interactions are highly nonlocal. The mechanism for error generation at wave numbers  $k \ll k_2$ , due to the small-scale 3-D turbulence, is basically the same as for the generation of the equilibrium range: errors are generated by beating interactions between wave numbers  $\sim k_2$  and are damped by eddy viscosity. We can, therefore, estimate the error spectrum (in the absence of large-scale motion) to be

$$(3.7) \quad E^{\text{err}}(k) \sim (k/k_2)^2 E(k_2) \sim (k/k_2)^2 l_2 v_2^2.$$

Errors generated by the small-scale turbulence will be enhanced by the instability of the large-scale flow, and most efficiently at wave numbers of the

order of the dissipation wave number  $k_{D,1}$ . The relative error is

$$(3.8) \quad r \sim E^{\text{err}}(k_{D,1})/E(k_{D,1}) \sim k_{D,1}/k_2.$$

We now assume exponential amplification of the error with a characteristic time equal to the turn-over time  $l_1/v_1$  in the enstrophy inertial range (roughly wave number independent); we find that the relative error has become of order unity after a time  $\sim t_1 \log(1/r) \sim t_1 \log(k_2/k_{D,1})$ . To this we must add the time for errors to migrate along the enstrophy inertial range from  $k_{D,1}$  to  $k_1$  which is  $\sim t_1 \log(k_{D,1}/k_1)$ . Hence the total predictability time is  $\sim t_1 \log(k_2/k_1)$ . In other words, thanks to the spectral gap, the predictability is the same as if we had a 2-D flow with full resolution of all scales down to the integral scale of the 3-D turbulence. The increased predictability can be rather important (days?) if a spectral gap exists at scales  $\sim 100$  km. This, of course, is debatable. It could be that the gap in the energy spectrum is filled by rare but violent meteorological events and does not exist in the mean; some increase in the predictability is then nevertheless expected.

Finally, we observe that coherent structures may play an important part in the dynamics of atmospheric turbulence. If this is so, predictability estimates based on turbulence phenomenology (*à la* Kolmogorov) may be very misleading.

\* \* \*

We have greatly benefitted from discussions with C. GLOAGUEN (two-component shell model) and with J. C. ANDRÉ, M. LESIEUR and O. THUAL (spectral gap and atmospheric predictability).

## APPENDIX

### **On the singularity structure of fully developed turbulence.**

with

G. PARISI

*Dipartimento di Fisica, Università di Roma II « Tor Vergata » - Roma, Italia*

A simple way of explaining power law structure function is to invoke singularities of the Euler equations considered as limit of the Navier-Stokes equations as the viscosity tends to zero. For Burgers' equation we know that such singularities exist (shocks) and that they provide the required explanation of scaling. For the 2-D Euler equations we know that singularities do not exist (see, *e.g.*, ref. [26] and references therein). For the 3-D Euler equations

the numerical evidence is inconclusive [26, 31]. MANDELBROT [24, 25] and others [20] have considered models with singularities concentrated on a set  $\subset \mathbf{R}^3$  having noninteger (fractal) Hausdorff dimension. We shall here show that the data suggest the existence of a hierarchy of such sets (a « multifractal »).

Since the Navier-Stokes equations (in the zero-viscosity limit) are invariant under the group of scaling transformations (defined in eq. (2.2)) for *any* value of  $h$ , singularities of arbitrary exponents (and mixtures thereof) are consistent with the equations. Specifically, we start with a definition, the velocity field at a given time  $v(x)$  is said to have a singularity of order  $h > 0$  at the point  $x$  if

$$(A.1) \quad \overline{\lim}_{x \rightarrow y} |v(x) - v(y)| |x - y|^h \neq 0.$$

For negative  $h$  eq. (A.1) is modified by not subtracting  $v(y)$ .

We call  $S(h)$  the set of points for which the velocity field has a singularity of order  $h$ . It is obvious that

$$(A.2) \quad S(h') \supset S(h) \quad \text{if } h' > h.$$

Roughly speaking,  $S(h)$  is the region where the velocity field is not an Hölder function of order  $h$ . We denote by  $d(h)$  the Hausdorff dimension of  $S(h)$  (see ref. [34] and [50] for definitions). It follows from eq. (A.2) that  $d'(h) > 0$ ; we also make the concavity assumption  $d''(h) < 0$ .

If such singularities exist, then, in the fully developed turbulence regime,  $d(h)$  has a nontrivial dependence on  $h$ : different kind of singularities are associated with sets having different Hausdorff dimensions. Note that the opposite phenomenon happens for the solutions of stochastic differential equations with white noise (like those studied in Jona-Lasinio's contribution to this volume): there the one-dimensional trajectories are (with probability one) Hölder functions of order  $\frac{1}{2}$ , so that

$$(A.3) \quad d(h) = \theta(h - \frac{1}{2}) \quad (\theta = \text{step function}).$$

It is useful to connect the function  $d(h)$  with the exponents  $\zeta_p$  introduced in eq. (2.4) which control the asymptotic behaviour of the longitudinal structure functions. We can try to rephrase the previous statements on the Hausdorff dimensions of  $S(h)$  by saying that the probability of having  $|v(x) - v(y)|$  of order  $|x - y|^h$  goes to zero like  $|x - y|^{3-d(h)}$  when  $|x - y| \rightarrow 0$ . We thus arrive to the following integral representation for the moments:

$$(A.4) \quad \langle (\delta v(l))^p \rangle \sim \int d\mu(h) l^{(p)h+3-d(h)},$$

where  $d\mu(h)$  is a measure concentrated on the region where  $d(h) > 0$ .

In the K 41 [18] picture and in the  $\beta$ -model [20], we have, respectively,

$$(A.5) \quad \begin{cases} \zeta_p = p/3, \\ \zeta_p = \lambda(p-3) + 1 \end{cases} \quad (\lambda < \frac{1}{3}).$$

Consequently we have, respectively,

$$(A.6) \quad \begin{cases} d(h) = 3\theta(h - \frac{1}{3}), & \text{K 41,} \\ d(h) = (2 + 3\lambda)\theta(h - \lambda), & \beta\text{-model.} \end{cases}$$

In more sophisticated models, and also in actual turbulence, according to ref. [29],  $\zeta_p$  is a nonlinear function of  $p$ . Evaluating the integral (A.4) using the saddle point method, we easily find

$$(A.7) \quad \zeta_p = \min_n [ph + 3 - d(h)].$$

We have thus found that  $\zeta_p$  is the Legendre transform (see ref. [51], sect. 14) of the codimension ( $c(h) \equiv 3 - d(h)$ ) of the set  $S(h)$ . This is assuring that the convexity properties of  $\zeta_p$  are automatically preserved by eq. (A.7).

If eqs. (A.4) and (A.7) are correct, the dimensions  $d(h)$  are experimentally well-defined quantities: they can be extracted from the  $\zeta_p$ 's by using the inverse Legendre transform

$$(A.8) \quad d(h) = 3 - \min_p (\zeta_p - ph).$$

We shall not try to do this using the data displayed in table I, although this is clearly possible, at least in the range of  $h$  for which the value of  $p$  minimizing eq. (8) falls in the experimentally observed interval: it is, however, likely that  $d(h)$  will not be a step function because  $\zeta_p$  appears to significantly deviate from a linear function of  $p$ . The function  $d(h)$  is thus nontrivial and singularities of different kinds, if they exist, are concentrated on sets having different Hausdorff dimensions.

The function  $d(h)$  (or, equivalently,  $\zeta_p$ ) has a clear dynamical meaning because it contains most of the relevant information on the scaling laws for fully developed turbulence. It would be rather important to measure accurately  $d(h)$  and to find good evidence for its universality, *i.e.* its independence on the initial conditions and on all the other parameters which should become irrelevant in the fully developed turbulence regime.

If the multifractal model is basically correct, accurate measurements of the  $\zeta_p$ 's may be quite difficult. Indeed, the structure functions are a mixture of power laws (eq. (A.4)), so that very small scales (*i.e.* very high Reynolds numbers) may be needed before the contribution with the smallest exponent clearly dominates; where exactly this happens depends on the distribution  $d\mu(h)$ .

Note that consistency of the multifractal model with the data is by no means evidence for real singularities of the Euler equations. There is certainly more than one way to obtain scaling, otherwise scaling would not be observed in two dimensions, where singularities are ruled out [26].

We note two interesting consequences of the inversion formula (A.8). First, if  $\zeta_p$  vanishes for  $p \rightarrow 0$ , then the weakest singularities, which has the exponent  $\zeta'_0$ , are space filling ( $d = 3$ ). It is clearly of interest to measure  $\zeta_p$  for small noninteger  $p$ 's. Second, the multifractal model is not completely consistent with Kolmogorov's [23] lognormal model for which  $\zeta_p = p/3 + \mu p(3-p)/18$  ( $\mu$ , if it exists, is somewhere between 0.2 and 0.5; see ref. [29]). Indeed, with this choice of  $\zeta_p$  we find from eq. (A.8) that beyond  $p_{\max} = 9(2/3\mu)^{1/2}$  a negative dimension is obtained. Accurate measurements of very-high-order structure functions are required to test for a possible inconsistency of the multifractal model.

Finally, one may wonder how the above « multifractal » model relates to the models of ref. [20, 25, 34, 52]. In Mandelbrot's [25, 34, 52] probabilistic models for the dissipation a random weighting factor  $W$  appears at each stage of the cascade. The case when  $W$  has a binomial distribution (« absolute curdling ») corresponds to a single fractal in our approach (it is also equivalent



to the  $\beta$ -model). For more general  $W$ -distributions (« weighted curdling ») one obtains exponents  $\zeta_p$  that depend nonlinearly on  $p$  like in the multifractal model. There is a single fractal for the energy dissipation, but it is conceivable that other fractals will be uncovered by investigating all possible singularities of the dissipation. Still the multifractal model appears to be somewhat more restrictive than Mandelbrot's weighted-curdling model which does include the lognormal case.

## REFERENCES

- [1] *Proceedings of « Nonlinear Dynamics »*, edited by H. G. HELLEMAN, *Ann. N. Y. Acad. Sci.*, **357** (1980).
- [2] *Proceedings of « Dynamical Systems and Chaos »*, edited by L. GARRIDO, *Lecture Notes in Physics*, Vol. **179** (Berlin, 1983).
- [3] *Proceedings of Les Houches, Session XXXVI, 1981*, edited by G. IOOSS, H. G. HELLEMAN and R. STORA (Amsterdam, 1983).
- [4] S. ORSZAG and A. PATERA: *Phys. Rev. Lett.*, **45**, 989 (1980).
- [5] M. BRACHET and S. ORSZAG: *Secondary instability of free shear flows*, to be published (1983).
- [6] D. RUELE: *Publ. Math. IHES*, **51** (1980).
- [7] G. BENETTIN, L. GALGANI, A. GIORGILLI and J. M. STRELCYN: *Meccanica* (Bologna, 1980), p. 9 and 21.
- [8] E. LORENZ: *Ann. N. Y. Acad. Sci.*, **357**, 282 (1980).
- [9] *Proceedings of « The Role of Coherent Structures in Modelling Turbulence and Mixing »*, edited by J. JIMENEZ, *Lecture Notes in Physics*, Vol. **136** (Berlin, 1981).
- [10] V. ARNOLD: *C. R. Acad. Sci.*, **261**, 17 (1965).
- [11] S. CHILDRESS: *J. Math. Phys. (N. Y.)*, **11**, 3063 (1970).
- [12] M. HÉNON: *C. R. Acad. Sci.*, **262**, 312 (1966).
- [13] H. AREF: *Stirring by chaotic advection*, *J. Fluid Mech.*, in press (1984).
- [14] P. COLLET and J. P. ECKMANN: *Iterated Maps on the Interval as Dynamical Systems* (Boston, 1980).
- [15] R. H. KRAICHNAN: *Phys. Fluids*, **10**, 1417 (1967).
- [16] R. H. KRAICHNAN: *J. Fluid Mech.*, **67**, 155 (1975).
- [17] H. K. MOFFATT: *Magnetic Field Generation in Electrically Conducting Fluids* (Cambridge, 1978).
- [18] A. N. KOLMOGOROV: *Dokl. Akad. Nauk SSSR*, **30**, 301 (1941).
- [19] G. K. BATCHELOR: *The Theory of Homogeneous Turbulence* (Cambridge, 1953).
- [20] U. FRISCH, P.-L. SULEM and M. NELKIN: *J. Fluid Mech.*, **87**, 719 (1978).
- [21] U. FRISCH and R. MORF: *Phys. Rev. A*, **23**, 2673 (1981).
- [22] G. K. BATCHELOR and A. A. TOWNSEND: *Proc. R. Soc. London, Ser. A*, **199**, 238 (1949).
- [23] A. N. KOLMOGOROV: *J. Fluid Mech.*, **13**, 82 (1962).
- [24] R. H. KRAICHNAN: *J. Fluid Mech.*, **62**, 305 (1974).
- [25] B. MANDELBROT: in *Turbulence and Navier-Stokes Equation*, edited by R. TEMAM, *Lecture Notes in Mathematics*, Vol. **565** (Berlin, 1976), p. 121.
- [26] U. FRISCH: in *Les Houches, Session XXXVI, Chaotic Behaviour in Deterministic Systems, 1981*, edited by G. IOOSS, H. G. HELLEMAN and R. STORA (Amsterdam, 1983).

- [27] R. H. KRAICHNAN: *Phys. Fluids*, **10**, 2080 (1967).
- [28] H. L. GRANT, R. W. STEWART and A. MOILLIET: *J. Fluid Mech.*, **12**, 241 (1962).
- [29] F. ANSELMET, Y. GAGNE, E. J. HOPFINGER and R. A. ANTONIA: *High order velocity structure functions in turbulent shear flows*, preprint Institut de Mécanique de Grenoble (1983).
- [30] M.-E. BRACHET: *C. R. Acad. Sci.*, **294**, 537 (1982).
- [31] M.-E. BRACHET, D. I. MEIRON, S. A. ORSZAG, B. G. NICKEL, R. H. MORF and U. FRISCH: *J. Fluid Mech.*, **130**, 411 (1983).
- [32] S. A. ORSZAG: in *Fluid Dynamics, Les Houches Summer School 1973*, edited by R. BALIAN and J. L. PEUBE (New York, N. Y., 1977), p. 235.
- [33] H. A. ROSE and P.-L. SULEM: *J. Phys. (Paris)*, **39**, 441 (1978).
- [34] B. MANDELBROT: *Fractals: Form, Chance and Dimension* (San Francisco, Cal., 1977).
- [35] R. GRAPPIN, J. LÉORAT and A. POUQUET: unpublished (1981).
- [36] C. GLOAGUEN: Thèse de 3ème Cycle, Observatoire de Meudon (1983).
- [37] V. N. DESNYANSKY and E. A. NOVIKOV: *Prikl. Mat. Mekh.*, **38**, 507 (1974).
- [38] T. L. BELL and M. NELKIN: *Phys. Fluids*, **20**, 345 (1977).
- [39] T. L. BELL and M. NELKIN: *J. Fluid Mech.*, **88**, 369 (1978).
- [40] E. SIGGIA: *Phys. Rev. A*, **17**, 1166 (1978).
- [41] R. M. KERR and E. SIGGIA: *J. Stat. Phys.*, **19**, 543 (1978). See also J. LEE: *J. Fluid Mech.*, **101**, 349 (1980).
- [42] A. POUQUET, U. FRISCH and J. P. CHOLLET: *Phys. Fluids*, **26**, 877 (1983).
- [43] E. LORENZ: in *Predictability of Fluid Motions*, edited by G. HOLLOWAY and B. WEST (American Institute of Physics, New York, N. Y., 1984), p. 133.
- [44] M. LESIEUR and D. SCHERTZER: *J. Méc.*, **17**, 610 (1978).
- [45] D. FORSTER, D. R. NELSON and M. STEPHEN: *Phys. Rev. A*, **16**, 732 (1977).
- [46] J.-D. FOURNIER, P.-L. SULEM and A. POUQUET: *J. Phys. A*, **15**, 1393 (1982).
- [47] D. McLAUGHLIN, G. PAPANICOLAOU and O. PIRONNEAU: *Convection of micro-structure*, preprint, Courant Institute, New York (1983).
- [48] E. LORENZ: *Tellus*, **21**, 289 (1969).
- [49] C. E. LEITH and R. H. KRAICHNAN: *J. Atmos. Sci.*, **29**, 1041 (1972).
- [50] J. P. KAHANE: in *Turbulence and Navier-Stokes Equation*, edited by R. TEMAM, *Lecture Notes in Mathematics*, Vol. **565** (Berlin, 1976), p. 94.
- [51] V. ARNOLD: *Mathematical Methods of Classical Mechanics* (Russian edition, Moscow, 1974; French edition, Moscow, 1976).
- [52] B. B. MANDELBROT: *J. Fluid Mech.*, **62**, 331 (1974).

Reprinted From  
 Turbulence and Predictability  
 in Geophysical Fluid Dynamics  
 and Climate Dynamics  
 © 1985, LXXXVIII Corso  
 Soc. Italiana di Fisica - Bologna - Italy